OAK RIDGE NATIONAL LABORATORY
operated by
UNION CARBIDE CORPORATION
for the
U.S. ATOMIC ENERGY COMMISSION

ORNL-TM-2774

COPY NO. - 1

DATE - Nov. 26, 1969

PRELIMINARY EVALUATION OF THE FIRST FUEL ROD FAILURE TRANSIENT TEST OF A ZIRCALOY-CLAD FUEL ROD CLUSTER IN TREAT

R. A. Lorenz, G. W. Parker and D. O. Hobson

ABSTRACT

The first fuel rod failure experiment in TREAT was performed September 12, 1969. The test was conducted as planned: all rods ruptured and fission products from the preirradiated center rod were collected on the two fission product collection systems. Only preliminary data are available from the post-experiment examination. Fission heating in the UO_2 pellets raised the Zircaloy cladding temperature of the 7-rod bundle 72°F/sec for about 20 sec. A variety of fuel rod construction including two clad alloys, different plenum volumes, different pellet-to-cladding clearances, and internal pressures ranging from 115 to 215 psia (77°F) were used.

The bundle was removed from its capsule and photographed in the hot cell. Photographs were taken of the bundle and of the individual rods after removal from their supports. Estimations of cooling channel blockage made from the photographs showed a maximum of approximately 58% blockage. The TREAT fuel rod failure tests utilize UO_2 pellets as the uniquely realistic heat source to duplicate precisely the internal heat transfer characteristics of actual power reactor fuel rods. Further examination of this first experiment is in progress, and the second experiment is being assembled.

CONTENTS

1.0 INTRODUCTION

The TREAT experiments simulate fuel rod failure under loss-of-coolant accident conditions for a PWR or BWR. This experiment used a 7-rod cluster of 27-in. long Zircaloy-clad UO_2 fuel rods with the center rod containing fission products from a 650 Mwd/ton irradiation in the MTR. Prepressurization of the rods with 115 to 215 psia helium (77°F) simulated fission gas released from a 10,000 Mwd/ton burnup. The fuel rod failure test was performed in TREAT by operating the reactor at steady power for about 20 sec so that fission heat in the 7-rod cluster raised the cladding temperature 72°F/sec. A flowing gas mixture of steam and helium carried fission products released from the center rod into two sequentially operated fission product collection systems. The first experiment was performed September 12, 1969, and a detailed description of the experiment design and a preliminary evaluation of the test results follows.

2.0 DESCRIPTION OF EQUIPMENT — TREAT FUEL ROD FAILURE EXPERIMENT FRF-1

2.1 General Description

A photograph of the in-reactor components of the equipment is shown in Fig. 2.1. Fuel rod cladding was a nominal 0.564 in. diameter and the rods were located on an equilateral triangle spacing 0.75 in. apart. The rods occupied 51% of the cross-sectional area in the triangular lattice and 46% of the area within the 2-3/16 in. I.D. Zircaloy sleeve surrounding the rod bundle. Steam flowed up through the rod bundle at a rate of 11 ℓ/min (STP) along with 1.8 ℓ/min (STP) helium at a pressure of about 19 psia. The steam-

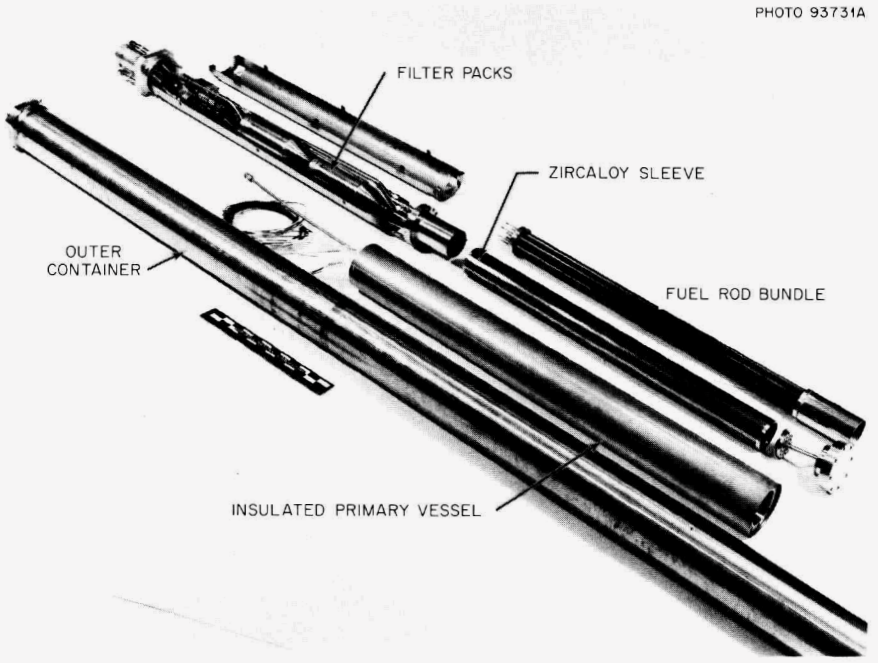

Fig. 2.1. In-Reactor Components of TREAT Fuel Rod Failure Experiment.

helium mixture carried fission products from the ruptured rods through the filter packs where most of the aerosol particles and iodine were collected. The entire steam system was preheated electrically to 130°C to prevent condensation of steam. The primary vessel was well insulated to prevent overheating of the reactor fuel when the experiment fuel rod bundle was heated to a much higher temperature.

The flow system is shown in Fig. 2.2. Constant heat input of 440 watts to the steam generator provided 9 g/min steam flow to the bottom of the rod bundle. Helium at 1.8 ℓ/min (STP) was mixed with the steam in the generator, and the mixture passed through a filter pack upon leaving the primary vessel. Chemically reactive compounds of the fission product iodine deposited on silver-plated surfaces and aerosol particles were collected on three fiberglass-asbestos filters in series. A high-efficiency silver-plated diffusion coil behind the filters trapped reactive iodine desorbed from particles on the filters. The steam was condensed and the helium carried remaining volatile fission products through a warm iodine-impregnated charcoal trap for collection of CH_3I and through liquid-nitrogen-cooled charcoal traps for collection of xenon and krypton. Effluent helium was monitored by rotameter and wet test meter. Hydrogen formed by reaction of steam with zirconium appeared as effluent gas flow greater than the controlled helium flow rate. A second identical fission product collection system was used after the first 90 sec in order to determine what fission products were slowly released after the initial rupture. Back-purging of Filter Pack No. 2 with helium prevented accidental contamination when Fission Product Collection Unit-1 was in use.

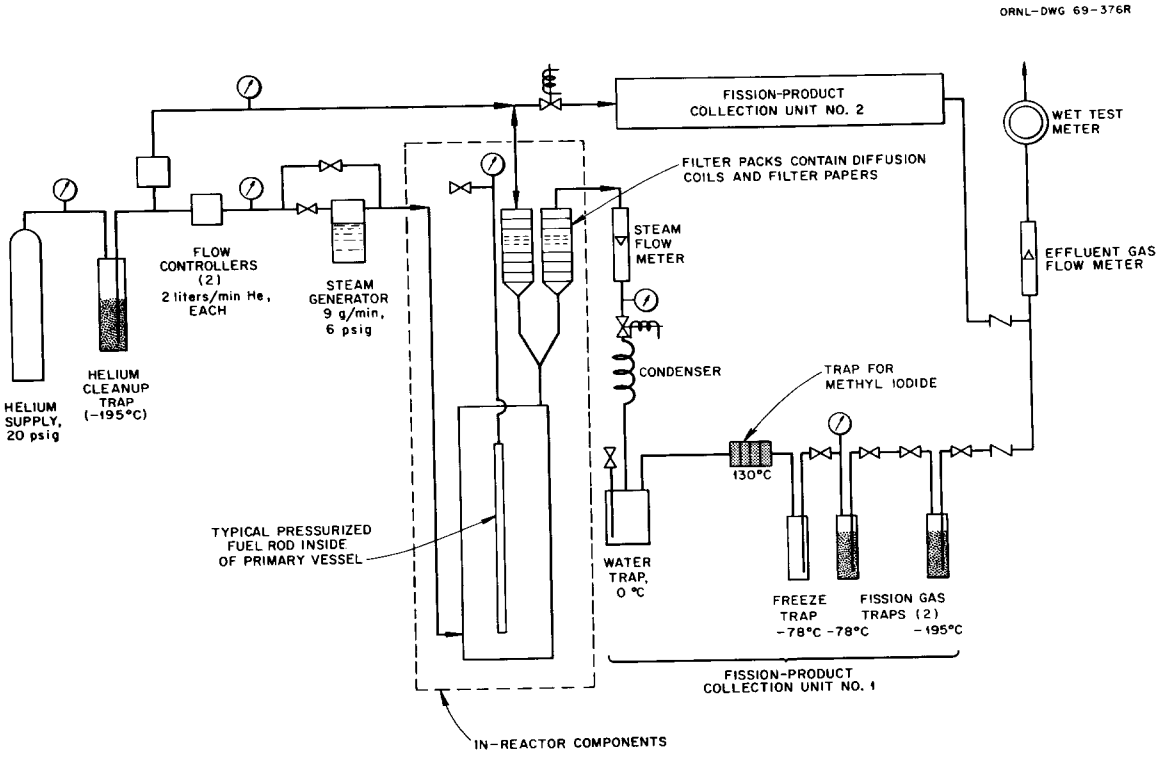

Fig. 2.2. Schematic Flow Diagram of TREAT Fuel Rod Failure Experiment.

2.2 Fuel Rod Construction

Details of fuel rod construction are given in Table 2.1. The four rods with Zircaloy-2 cladding were surplus rods of commercial manufacture built to Dresden-I dimensions. The rods were used "as-received" so that precise internal dimensions are not yet available. Nominal dimensions were: cladding, 0.564 in. dia and 0.033 in. wall thickness, and UO_2 dia 0.492 in. The three rods with Zircaloy-4 cladding were assembled at ORNL using cladding of recent commercial manufacture. All rods had a combined fuel and plenum length of 26-7/8 in. Selected pellets from extra "Dresden-I" rods were used for fuel. The pellets averaged 0.62 in. long and had an O/U ratio of 2.001. The immersion density at 25°C in water averaged 10.34 (94.4% of theoretical), enrichment was 1.51%, and impurities were less than 100 ppm for each element identified. All cladding was inspected ultrasonically for flaws using a 0.002 x 0.002 x 0.5 in. groove as a standard. No defects were detected in these rods although most of the rods from the Dresden-I size batch showed defects. The plenums of the three Zircaloy-4 rods each contained a spring wound from 1/16 in. dia Zircaloy wire. The spring deflection was 0.12 in./in.-lb, but the rods were assembled without compression on the springs. A 3/8 in. long Zircaloy cylinder with a 1/16 x 1/16 in. groove for free gas passage was located between the spring and first pellet.

A 1/8 in. dia Zircaloy tube with 1/16 in. dia hole was welded to the top of each rod for pressurizing. The rods were held at 255°F and evacuated overnight for drying and outgassing. The void volume was measured by expanding helium into the rod from a known volume. Pressure was increased to the desired level and the tube was pinched from the outside onto a 1/16 in. dia gold wire located in the tube. The pinch-seal was checked for leakage and the tube then cut and seal welded. A final leak check was made with a mass

Table 2.1. Fuel Rod Characteristics

ROD IDENTIFICATION:	CENTER	4-1	4-2	R	I	H	L
Cladding Material:	Zr-4	Zr-4	Zr-4	Zr-2	Zr-2	Zr-2	Zr-2
Cladding, O.D., in.	0.5637	0.5638	0.5638	~0.564	~0.564	~0.564	~0.564
Cladding, I.D., in.	0.4986	0.4989	0.4989				
Wall Thickness, in.	0.033	0.033	0.033	~0.033	~0.033	~0.033	~0.033
Pellet Dia., in.	0.488/0.489	0.496/0.497	0.496	~0.492	~0.492	~0.492	~0.492
Pellet Length, in.	5/8	5/8	5/8				
Gross Wt., g	965	1023	975	1074	1038	1096	1094
UO_2 Wt., g	766	820	767	884	848	906	905
Plenum Length, in.	2-5/8	1-1/8	3-5/16	0	0	0	0
Plenum Volume, cm^3	7.55	3.23	9.51	0	0	0	0
Clad Gap and Pellet Gap Voids, cm^3	3.54	2.74	1.45	4.01	7.18	2.5	2.9
Pressure Cell and Tubing, cm^3	0	0	0	0	0	~3.0	~3.0
Total Gas Space, cm^3	11.09	5.97	10.96	4.01	7.18	5.50	5.92
Pressure, psia He at 25°C	215	215	215	215	115	133	207
Helium in Rod, cm^3 (STP)	149	80	147	54	52	46	76

spectrometer helium leak detector. After assembly, the Zircaloy-4 rods were autoclaved for 2 days in 1500 psi steam at 750°F. The helium fill pressure range of 115 to 215 psia (77°F) was based on estimates of fission gas pressure in a BWR calculated by the D′ (empirical) method.[1] This calculation showed that most of the rods would contain pressure below this range, but that most of the volatile fission products released from UO_2 into the rod void spaces would be contained in rods with pressures above this range.

The differences in rod construction were made to see if any one variable strongly influenced the characteristics of clad swelling and rupture. Two cladding alloys were used, pellet to clad gap ranged from 0.002 to 0.010 in. on the diameter, total void volume ranged from 4.0 to 11.1 cm^3, and internal pressure ranged from 115 to 215 psia (77°F). Rods H and L were each connected to a strain gauge pressure transducer for continuous monitoring of internal pressure. Both rods had two Pt vs Pt-Rh thermocouples made of 30 gauge wire spot-welded to the cladding, but two of these thermocouples, one on each rod, were damaged after initial assembly when alterations were made to allow increased linear expansion.

2.3 Fuel Rod Suspension

Rods H and L, which were connected to pressure cells, were hung from the top support spider and tightened to the spider so that rotation or other movement at that location would be highly restrained. These rods and all others had 1/32 in. clearance on the dia with the bottom spider spacer. The other rods rested on a bottom support plate without any restraint on rotation. The top end of these rods had 1/64 in. clearance on the diameter in holes in the upper support spider. All rods had 5/16 in. available for linear expansion. The rods were not clipped or supported other than at the ends.

2.4 Center Rod Irradiation

The center rod was placed in a special irradiation capsule and irradiated as experiment ORNL-58-2 in the MTR from June 11 to June 25, 1969, for 13.125 full power days. The design linear power heat rating for the irradiation was 15 kw/ft avg which was the same as the hotter rods of a modern BWR. Magnesium alloy spacers between the rod and outer stainless steel container provided the proper temperature drop between the fuel rod cladding and the relatively cool MTR cooling water. After the irradiation the rod was neutron radiographed and gamma scanned with a lithium-drifted germanium scintillation crystal and a 0.005 in. slit-width collimator. The neutron radiograph showed that a central void did not form in the UO_2 pellets. An axial void would be expected from grain growth and sintering with sufficient time at temperatures above 1900°C. The gamma scan showed uniform fission product concentrations at pellet centers and at pellet interfaces. Previous experience with a group of special capsules showed a correlation between high heat rating, central void formation and the presence of radiation peaks at pellet interfaces caused by migration of fission products.[2,3] After gamma scanning, the rod was removed from its irradiation capsule and installed in the center of the TREAT experiment bundle in the TAN (Test Area North) hot cells at the National Reactor Testing Station.

3.0 EXPERIMENTAL PROCEDURE

The experiment was installed in TREAT, the entire flow system was tested with 30 psig helium for leakage, flow control valves were tested and the steam safety shutoff system was tested. Two calibration transients were performed at low reactor energy output to confirm the calculated rise in cladding

temperature for a given reactor energy release. The first calibration transient was performed with the experiment evacuated and initially at room temperature to minimize heat loss. The second transient was performed with steam flow and the experiment preheated. Temperature response to the three transients is summarized in Table 3.2. The increase in primary vessel temperature resulted from reactor gamma heating.

The loss-of-coolant transient proceeded according to the following schedule:

-14 min	Steam flow started (11 ℓ/min STP), helium flow: 1.8 ℓ/min (STP) through primary vessel and 1.8 ℓ/min (STP) additional purge through Filter Pack-2.
0 min	Start of TREAT transient.
8 sec	Reactor power steady at 30 Mw.
28 sec	Reactor power decreasing from 30 Mw Rods H and L rupture. Maximum measured cladding temperature of 1770°F reached. Primary vessel pressure increase from 7.6 to 10.5 psig caused mainly by helium released from rods.
90 sec	Flow changed to Fission Product Collection Unit-2.
10.5 min	Heat to steam generator turned off.
16.25 min	Flow changed back to Unit-1.
18 min	Steam generator bypassed.
30 min	Flow stopped.

Table 3.2. Temperature Response to Reactor Transients

		TREAT Integrated Power Mwsec	Duration of Reactor Power sec	TC-7 (Rod H) °F	TC-9 (Rod L) °F	TC-3 (Primary Vessel) °F
Calibration Transient #1:	Start	0	0	94.6	95.4	84
	End	38.9	2	229.5	233.6	86
Calibration Transient #2:	Start	0	0	365	365	327
	End	195.3	10	918	903	343
Loss-of-Coolant Transient:	Start	0	0	361	356	331
	End	556	20	1771	1679	388

4.0 EXPERIMENTAL RESULTS

4.1 Data Obtained During In-TREAT Experiment

Measured reactor power, cladding temperature and rod internal pressures are shown in Fig. 4.3. TC-7 was 9-5/16 in. below the top of rod H at a location receiving 99% of the peak flux. TC-9 was 6-1/4 in. below the top of rod L where the flux was about 94% of the peak. The cladding temperature rate of rise averaged 72°F/sec. Pressures in rods H and L are shown as recorded without any correction for zero bias or zero shift due to temperature or radiation. The initial pressures in rods H and L preheated to 300°F should have been 189 and 293 psia, respectively, and the pressures after rupture should have been equal to the primary vessel pressure, 23 psia. Peaking of the pressure curves at 23 sec (1560°F) probably corresponds to the beginning of significant volume increase by swelling. The pressure increase in these two rods should have been slower than in other rods because of the unheated gas volume in the tubing and pressure cell.

System pressures and flow rate are shown in Fig. 4.4. Primary vessel pressure was obtained from gauges located outside of the reactor so that response was slow. A sensitive pressure cell located close to the primary vessel failed during mockup testing and could not be replaced. Therefore the individual pressure pulses from rupturing rods were not obtained. The large rise in pressure between 25 and 30 sec indicates that most of the rods failed within this time span. The decrease in primary vessel pressure at 90 sec when flow was changed is a result of less flow restriction in Unit-2. The gradual rise in pressure after 150 sec is undoubtedly due to a buildup of flow restriction in one of the freeze traps. Increased flow rate of steam leaving the primary vessel between 25 and 35 sec results from higher

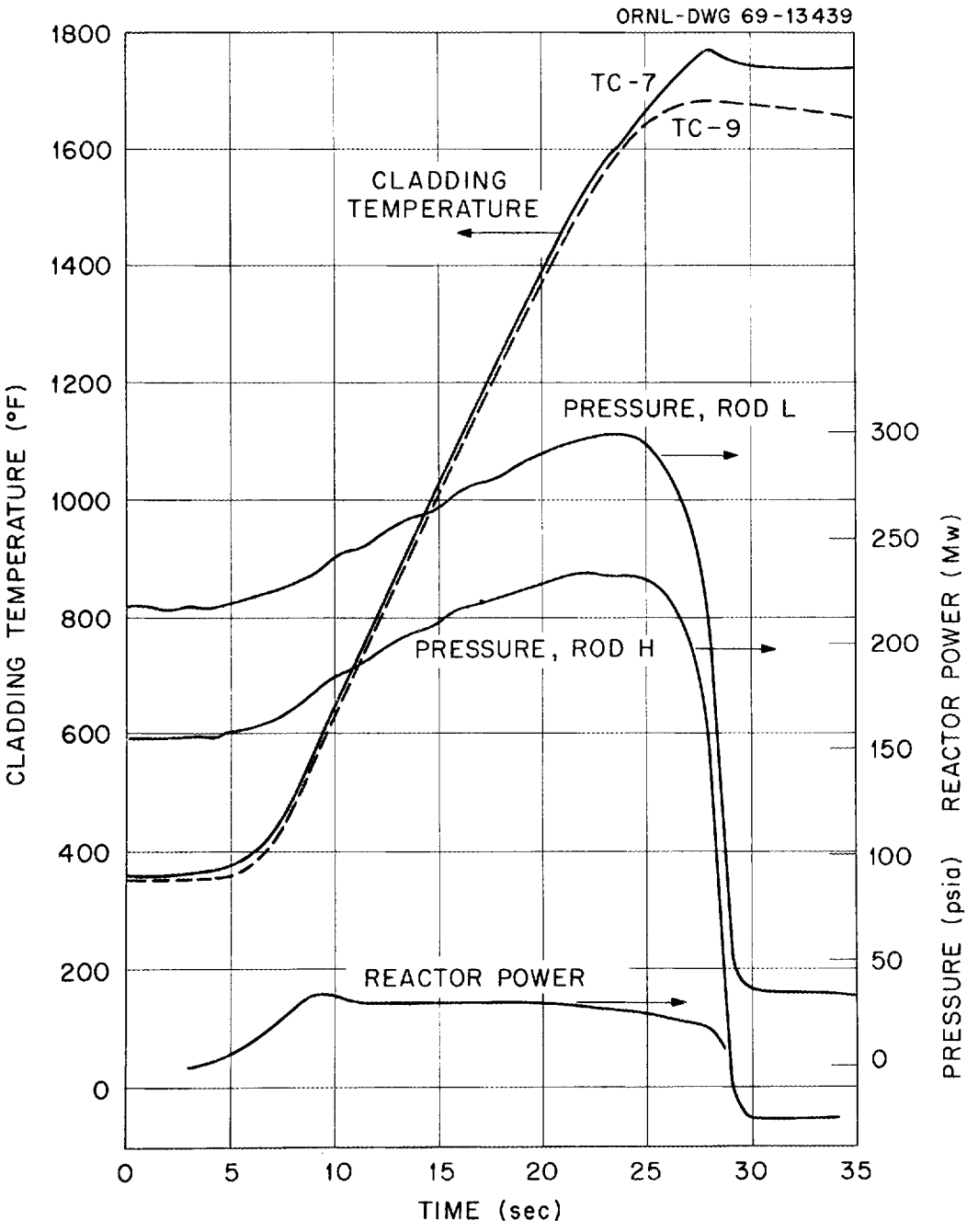

Fig. 4.3. Fuel Rod Temperatures and Pressures in TREAT Experiment FRF-1.

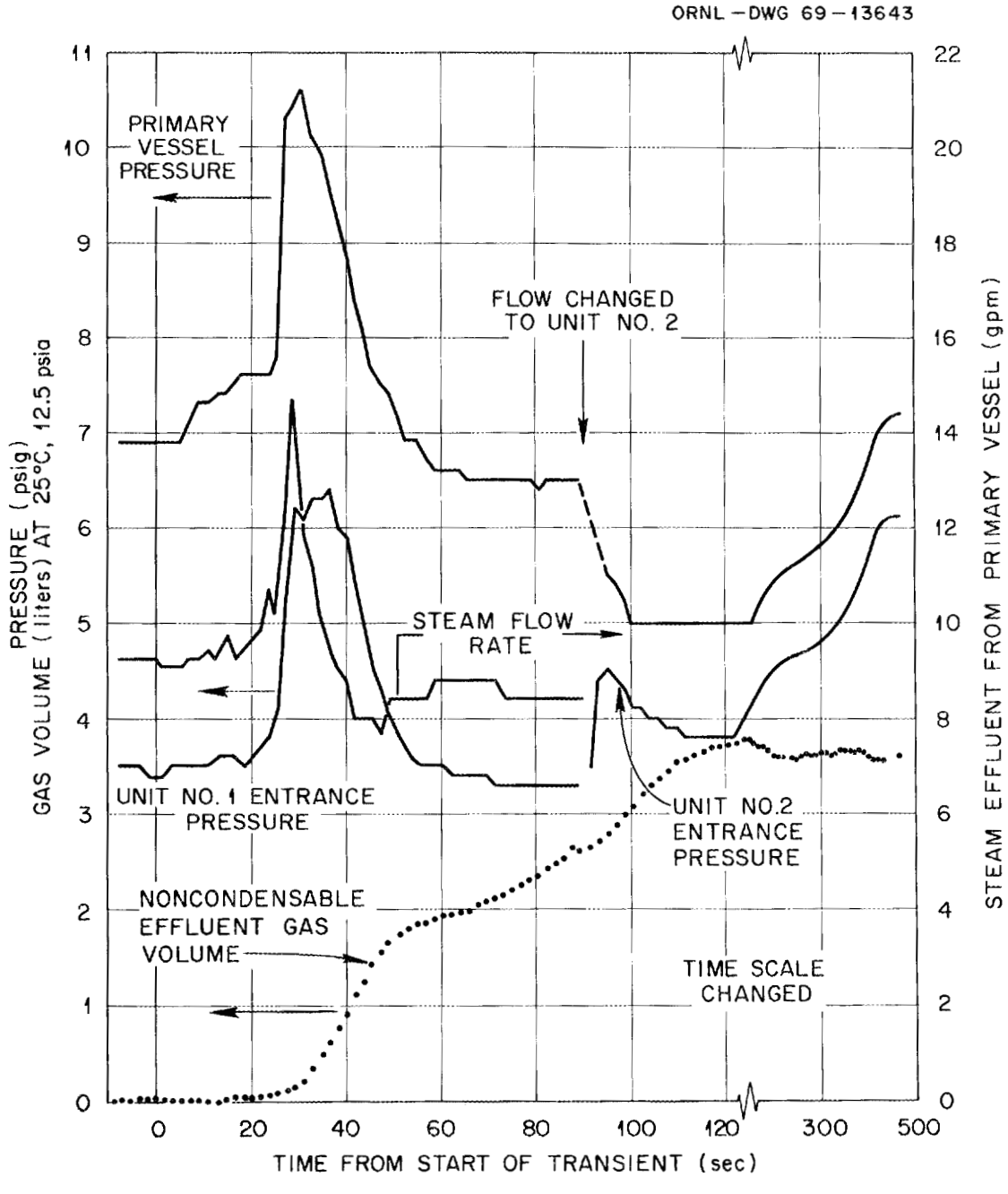

Fig. 4.4. System Pressure and Flow Rate During TREAT Fuel Rod Failure Experiment FRF-1.

pressure in the primary vessel. The slightly lower flow rate between 36 and 60 sec may represent a conversion of steam to hydrogen. This reaction is on a 1-to-1 volume ratio, but the rotameter does not respond significantly to hydrogen because of its low density.

The wet test meter at the outlet of the flow system measures combined helium and hydrogen flow. The effluent gas volume curve in Fig. 4.4 was obtained from wet test meter readings with the constant helium flow subtracted. No correction was made for the effect of temperature increase or pressure changes in the primary vessel, or for helium released from the rods. The volume of helium released from the rods was 775 cm^3 at 12.5 psia and 77°F, the ambient conditions of the wet test meter. Temperature and pressure changes in the system account for about 1.3 liters of helium effluent between times 0 and 120 sec. Therefore we estimate the volume of hydrogen generated by metal-water reaction to be 1.2 ± 0.6 liters (STP). This is equivalent to about 0.3% metal-water reaction based on total cladding volume.

4.2 Fission Product Release

All of the planned samples have been submitted for radiochemical analysis, but only 10% of the analyses have been returned. In general, the fission product collection systems functioned as planned and the distribution of fission products was as expected. Iodine and cesium were the principal components of an NH_4OH rinse of the primary vessel. The diffusion coils showed the ^{131}I gamma spectrum above a "fuel" spectrum. The first filter of Unit-1 is shown in Fig. 4.5 and showed a strong "fuel" gamma spectrum. The screen pattern is from a covering screen. The second and third filters appeared clean but contained a small amount of ^{131}I. The backup diffusion coil also collected some ^{131}I. Loose particles, probably fuel from some of the outer rods,

Fig. 4.5. First Filter of Fission Product Collection Unit-1, TREAT Experiment FRF-1.

collected around the entrance screens and diffusion coils of Unit-1. The Unit-2 filter pack did not contain visible particles.

The steam condensate contained a trace of ^{131}I, and more ^{131}I was found in the heated charcoal traps. ^{85}Kr, ^{131m}Xe, and ^{133}Xe were found in the cold charcoal traps. Total fission product release was somewhat less than expected, reflecting the short (13-day) irradiation of the center rod and possibly a linear power rating lower than requested.

Some volatile short half-life fission products were collected on the charcoal traps. These fission products were formed during the TREAT transient and may be useful as a measure of the "heating burst." The "heating burst" is the amount of fission gas above that expected by diffusion when UO_2 is first heated.[4] TREAT-generated fission products would be released mainly by heating and cooling bursts, but MTR-generated fission products would be released from UO_2 by diffusion and recoil in the MTR as well as by heating and cooling bursts in TREAT. Diffusion in the MTR is meant to include release by grain growth and other postulated high-temperature release mechanisms. The short half-life fission products were identified by following the decay rate since quantitative gamma spectrometric analysis could not be arranged at the late hour of loss-of-coolant transient. ^{134}I and ^{135}I were identified in the heated charcoal trap and ^{87}Kr and ^{88}Kr were the predominant short half-life fission products in the rare gas charcoal traps.

4.3 General Description of the Bundle as Removed from the Capsule

The experiment was dismantled in the TAN facility hot cells. The bolts holding the top end-cap were unscrewed and the capsule was upended to slide the rods part way out of the capsule. Photographs were taken of the rods as they were

removed to illustrate the relative positions of the ruptures and the overall appearance of the rupture region. The fields of view of the various photographs are illustrated in Fig. 4.6. The photographs, Figs. 4.7 through 4.16, show that the ruptures occurred on the inside of the rod bundle. It must be presumed that the inside of the bundle was hotter than the outside due to the relatively cooler outer sleeve. Figures 4.7 and 4.8, taken from approximately the same positions, show a small fragment of cladding from the rupture region of the center rod. Figure 4.9 is an overall view of the partially removed bundle taken at the same angle as Fig. 4.8. The small cladding fragment seen in the two previous figures is no longer seen and has presumably fallen to the hot cell floor during handling of the assembly. Figure 4.10 shows the closest approach, except for point contact between a rupture and an adjacent rod, of any of the rods along any appreciable length of the bundle. Figures 4.11 and 4.12 are two other views taken around the bundle.

We realize that the positions of the rods in the bundle before and after removal from the capsule may differ. Because there was considerable bowing of the rods during the test, and because such bowing could have been elastically restrained by the surrounding Zircaloy sleeve, the rods may have been in more intimate contact than is shown in the photographs.

Figure 4.13 is an overall view of the bundle taken at a point opposite Fig. 4.9. Figure 4.14 is a composite showing the bulge in the center rod and the entire length of the rupture zone of the bundle. Figure 4.15 shows the rupture in rod R straddling rod 4-2. Figure 4.16 shows the center rod after removal of rod 4-1. The relative positions of the rods in this photograph were shifted when 4-1 was removed.

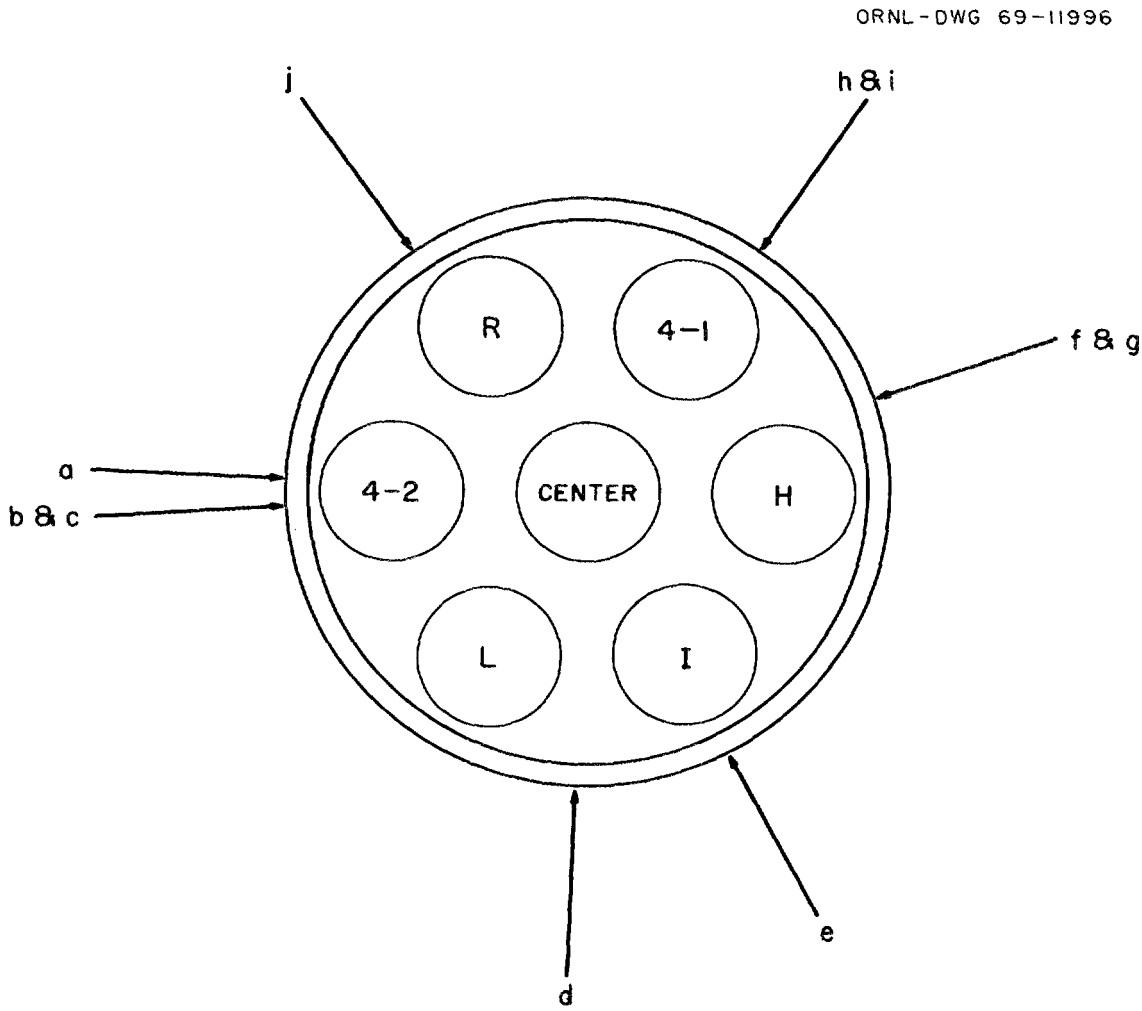

Fig. 4.6 Diagram of the Cross Section of the TREAT Bundle Illustrating the Directions (a through j) From Which Photographs Were Taken. The diagram represents the bottom of the rod cluster, but it is also the view of the upended bundle as seen from the top of the hot cell.

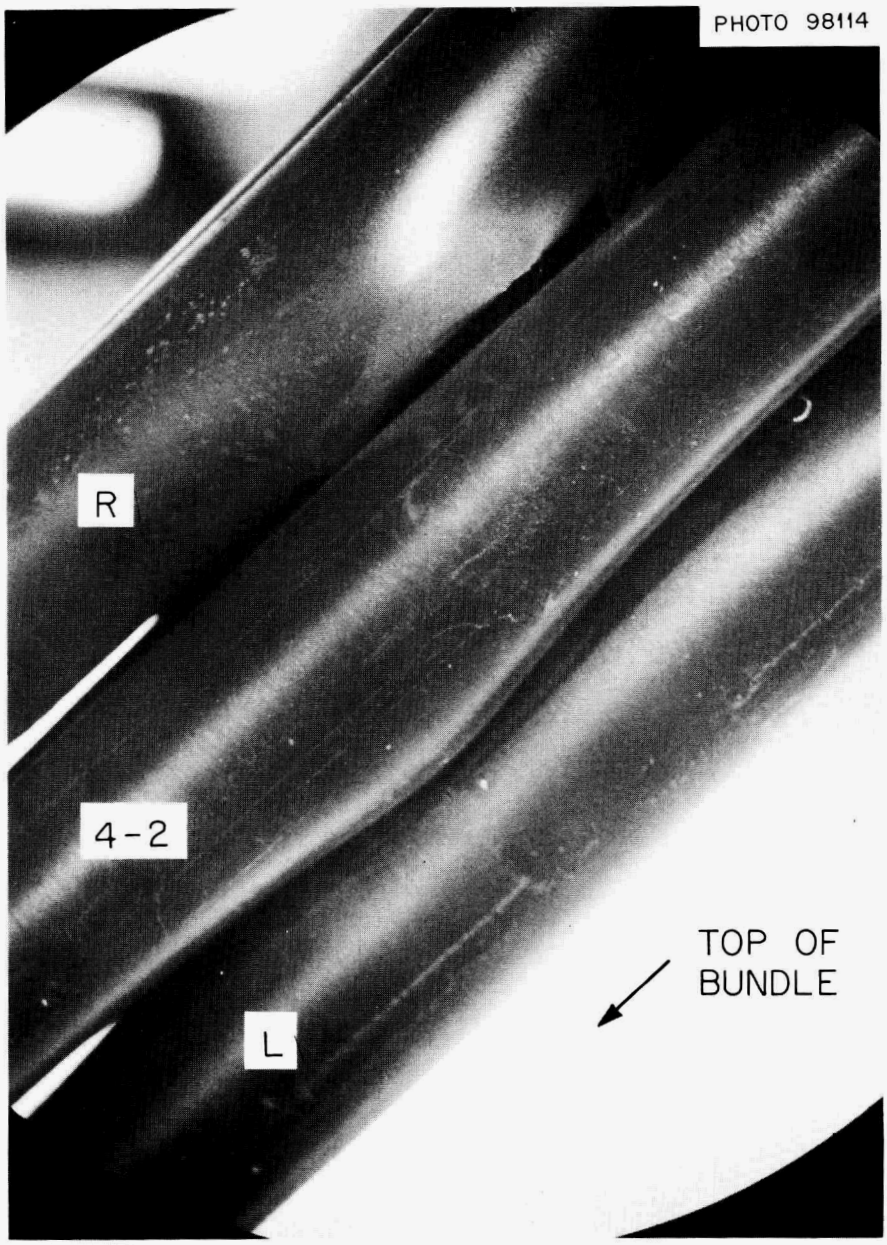

Fig. 4.7 Periscope View (a) of Rods R, 4-2 and L (left to right). The rupture in rod R is visible as well as the cladding fragment from the center rod rupture.

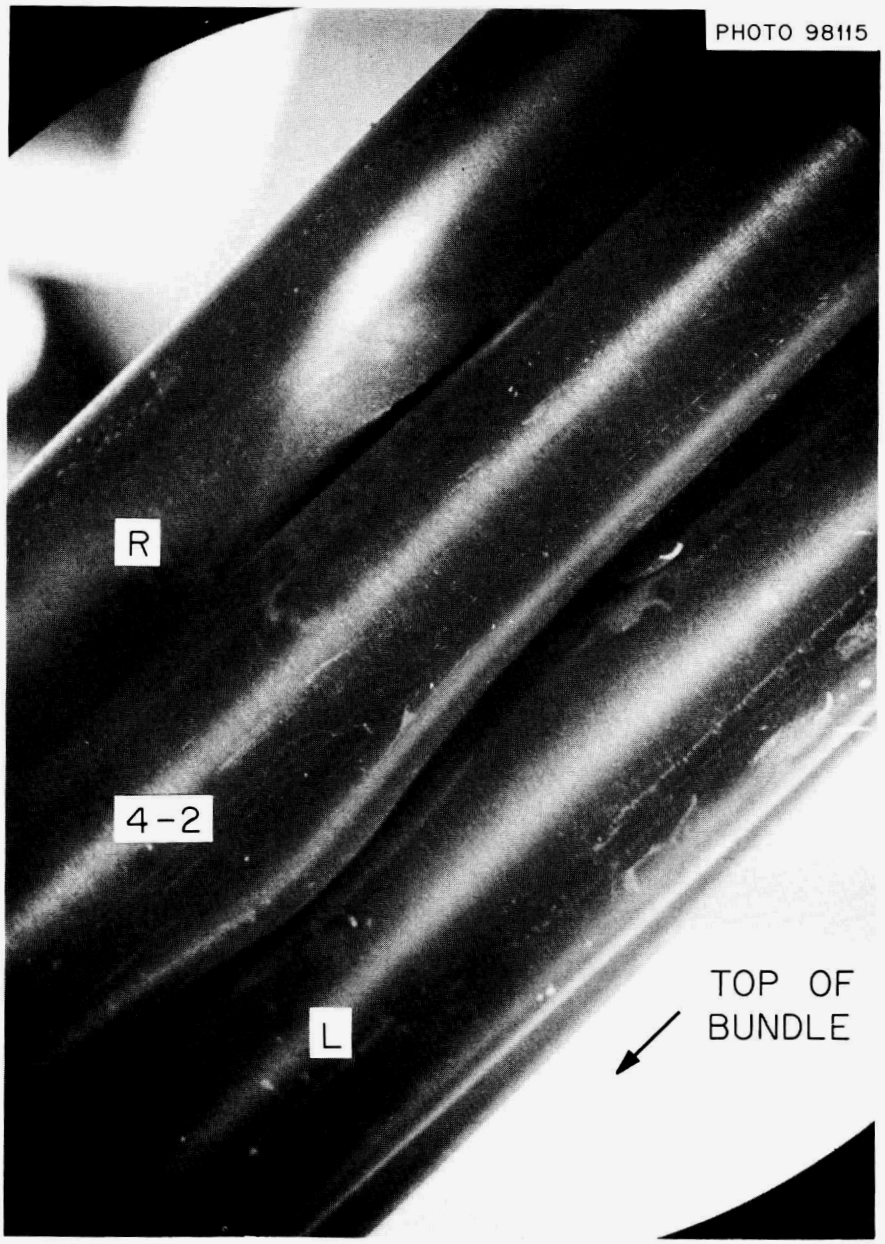

Fig. 4.8 View (b). Same as Fig. 7, Except for Slight Rotation of the Bundle to Allow Better Examination of the Fragment.

Fig. 4.9 View (c). Overall View of the Bundle After Approximately 75% Withdrawal From the Capsule. The rupture region is visible near the center of the photograph.

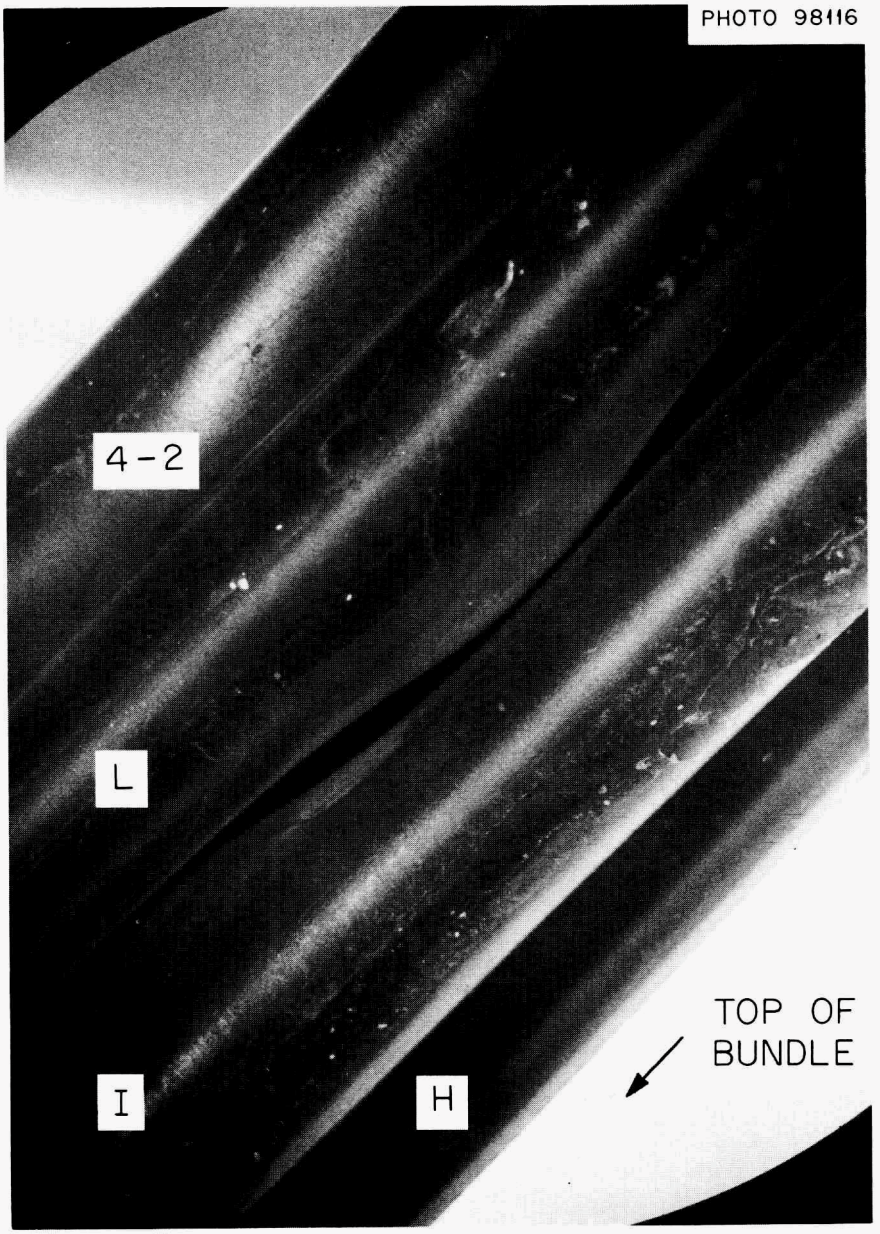

Fig. 4.10 View (d). Photograph of Rods 4-2, L, I and H (left to right). The close approach of Rods L and I is apparent.

Fig. 4.11 View (e). Photograph of Rods L, I and H.

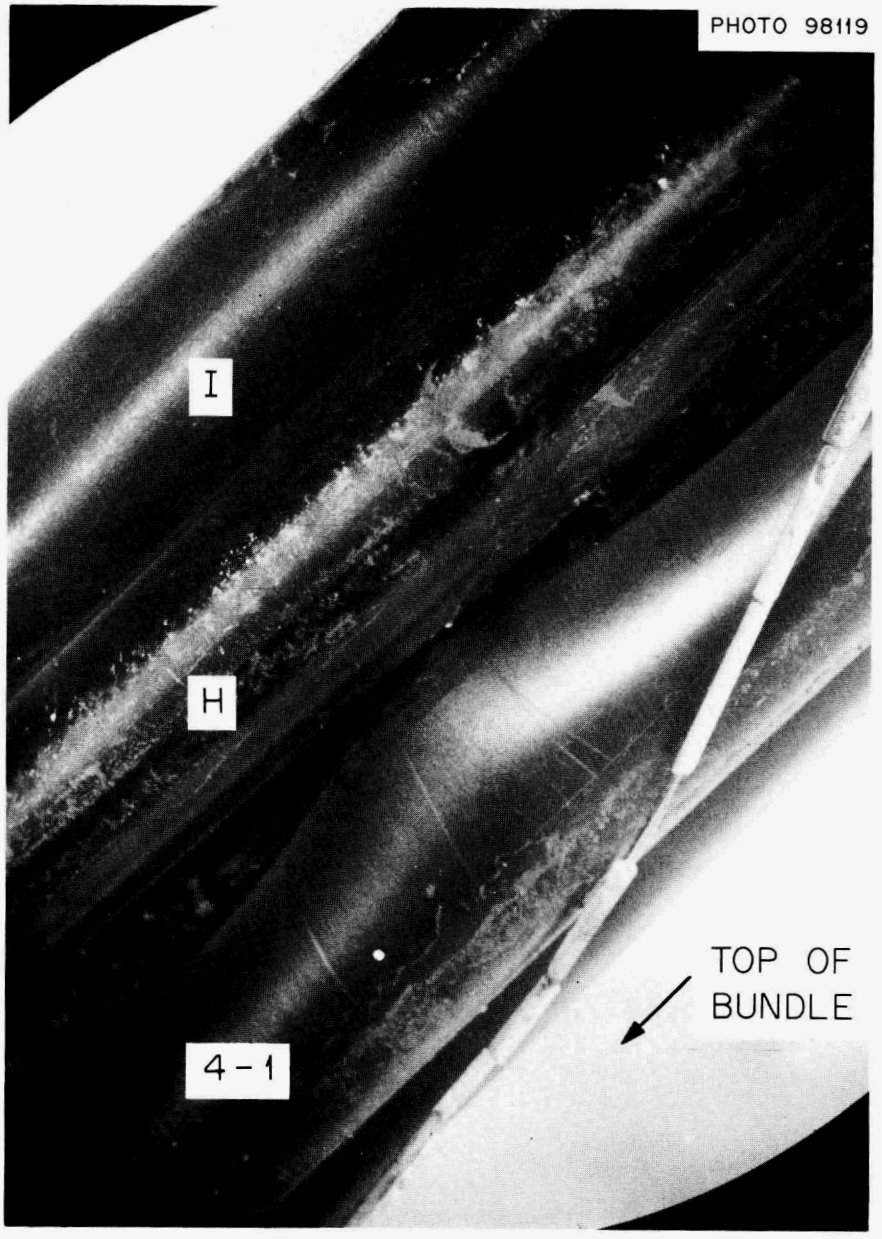

Fig. 4.12 View (f). Photograph of Rods I, H, 4-1 and R. The center rod is just visible.

Fig. 4.13 View (g). Overall View of the Bundle Approximately 180° from Fig. 4.9.

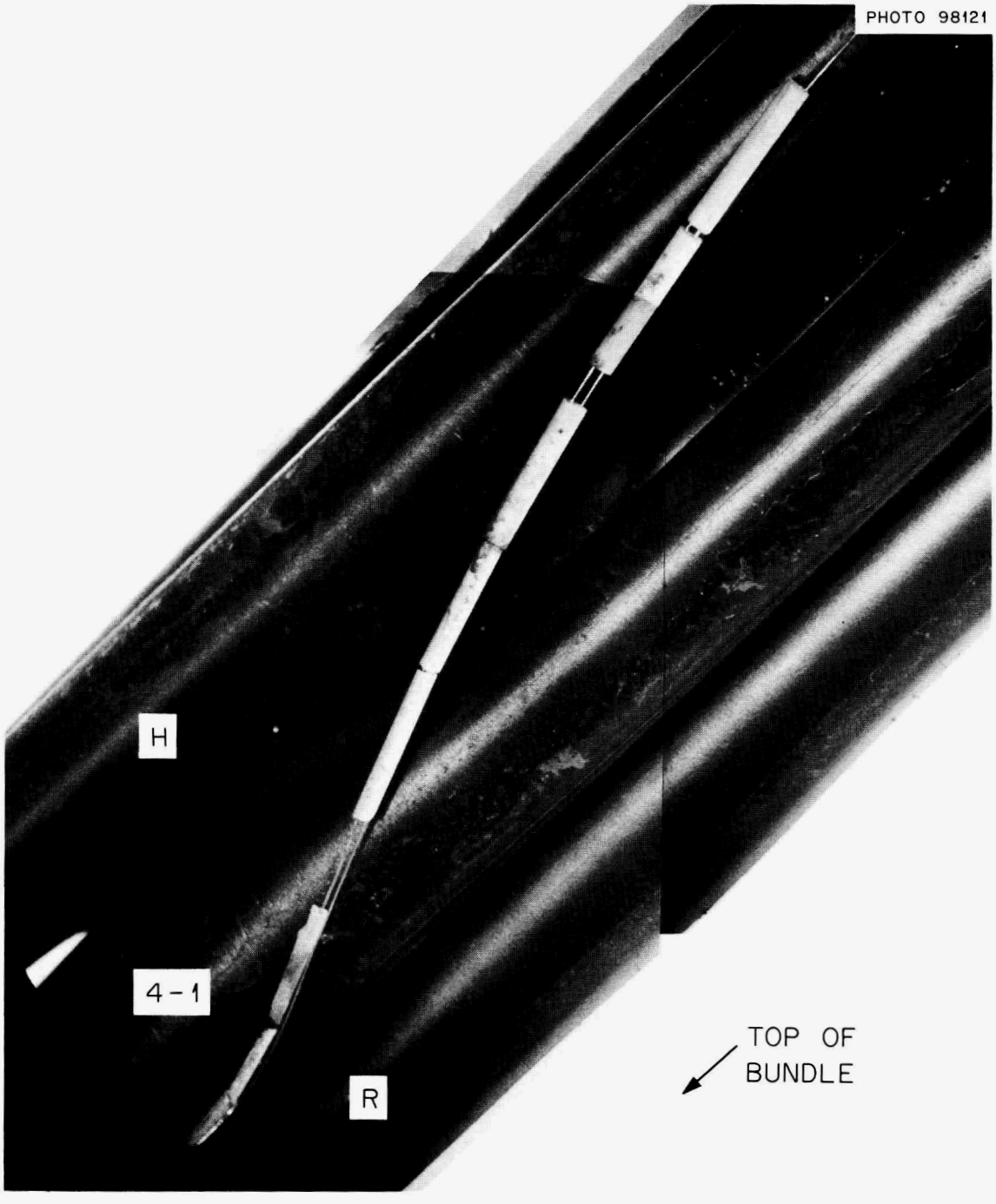

Fig. 4.14 Views (h and i). Photographs of Rods H, 4-1 and R. A portion of the rupture bulge in the center rod is visible. Two photographs have been mounted to show the entire length of the rupture zone of the bundle.

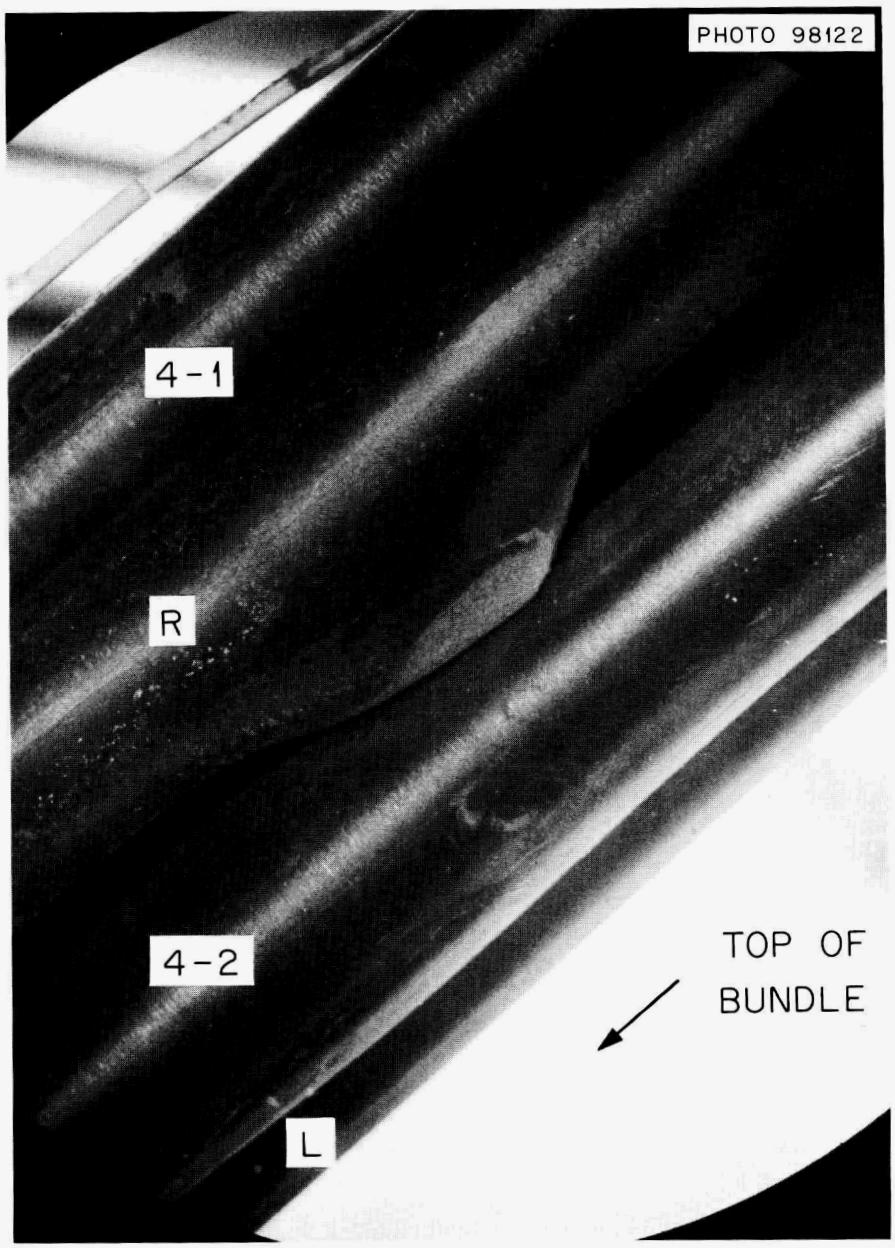

Fig. 4.15 View (j). Photograph of Rods 4-1, R, 4-2 and L Showing the Rupture in Rod R Straddling Rod 4-2.

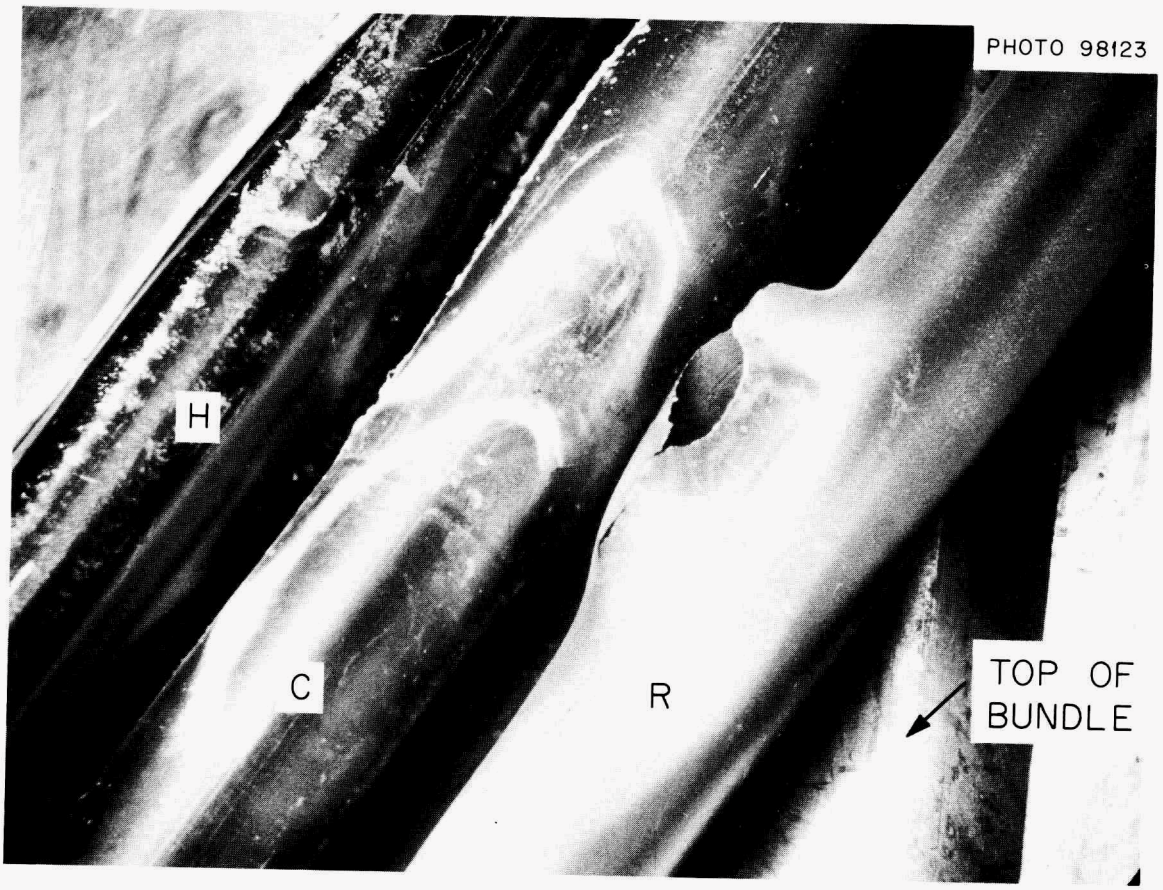

Fig. 4.16 Photograph of Rods H, Center and R After Removal of Rod 4-1. Rod R has been rotated approximately 120° from its burst position.

4.4 General Description of the Rods

The bundle was further dismantled and the rods were laid out and photographed both in plan and in elevation at the rupture. A montage is shown in Figs. 4.17 and 4.18. The horizontal background lines represent one inch intervals down the lengths of the rods and are referenced to the top shoulders of the rods. The numbers associated with the rods are diametral expansions in percent measured in plan and elevation. The rods are arranged so that the ruptures are in the correct axial positions relative to one another. All ruptures occurred within less than two inches axial distance along the bundle. It was apparent that rod rotation occurred between individual rod bursts. It was impossible to find a single overall position for the seven rods that could explain all of the burst markings on the rods. Future TREAT experiments will be run with the rods pinned so that rotation cannot occur.

The rods were examined for bowing by placing them against a large, vertical sheet of graph paper so that the maximum bowing was perpendicular to the axis of view through the window of the hot cell. The rods were photographed and the amounts of bowing and the positions of the rod ruptures were measured on the graph paper. Figure 4.19 illustrates the rods in position against the graph paper. The maximum bowing occurred in rod H. The surface at the point of maximum concavity, opposite the rupture, underwent a lateral displacement of approximately 0.235 inches. Both bowing and swelling contributed to this displacement. Assuming a swelling of 30%, based on uniform swelling and neglecting the rupture bulge, it was calculated that the rod axis was displaced approximately 0.15 inches from its original centerline. Since the maximum radial clearance between the rods and the Zircaloy sleeve was approximately 0.060 inches, it is probable that either the rods started bowing, hit the sleeve and then

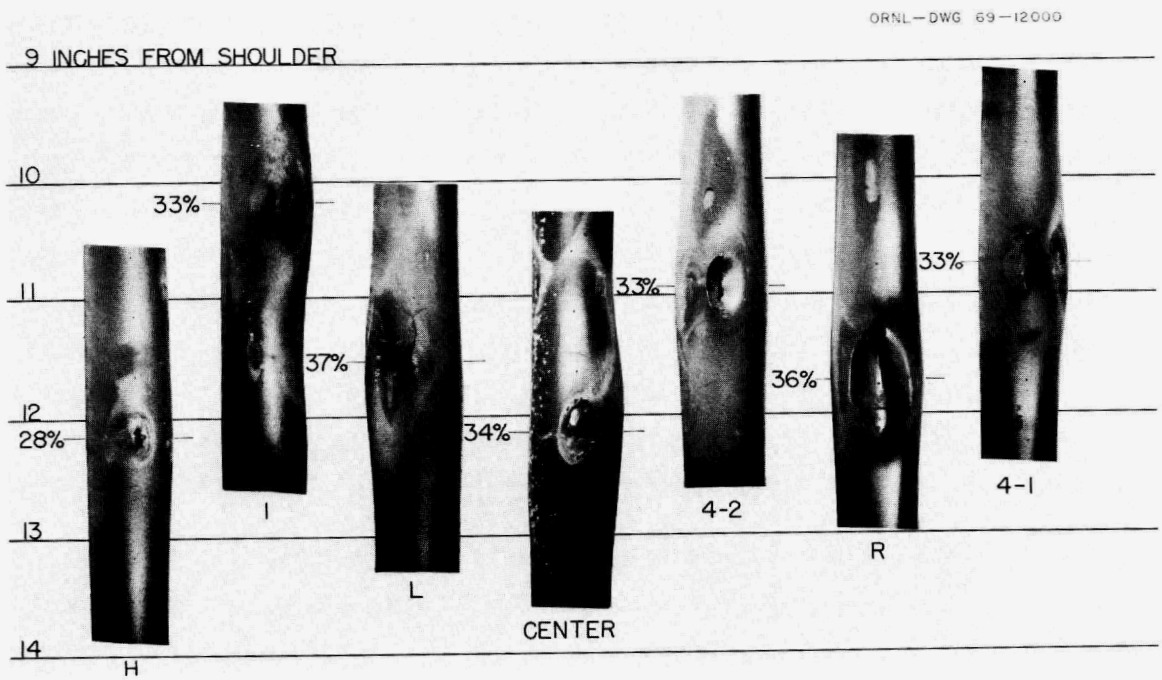

Fig. 4.17 A Montage Showing Plan Views of the Ruptures in the Rods. The ruptures are in their correct axial positions relative to one another. The percentage figures represent maximum diametral expansion. Rod 4-2 shows a thick powder buildup on the same level as the rupture in rod I. Rod R shows traces of the same powder. The powder was reddish-brown in color.

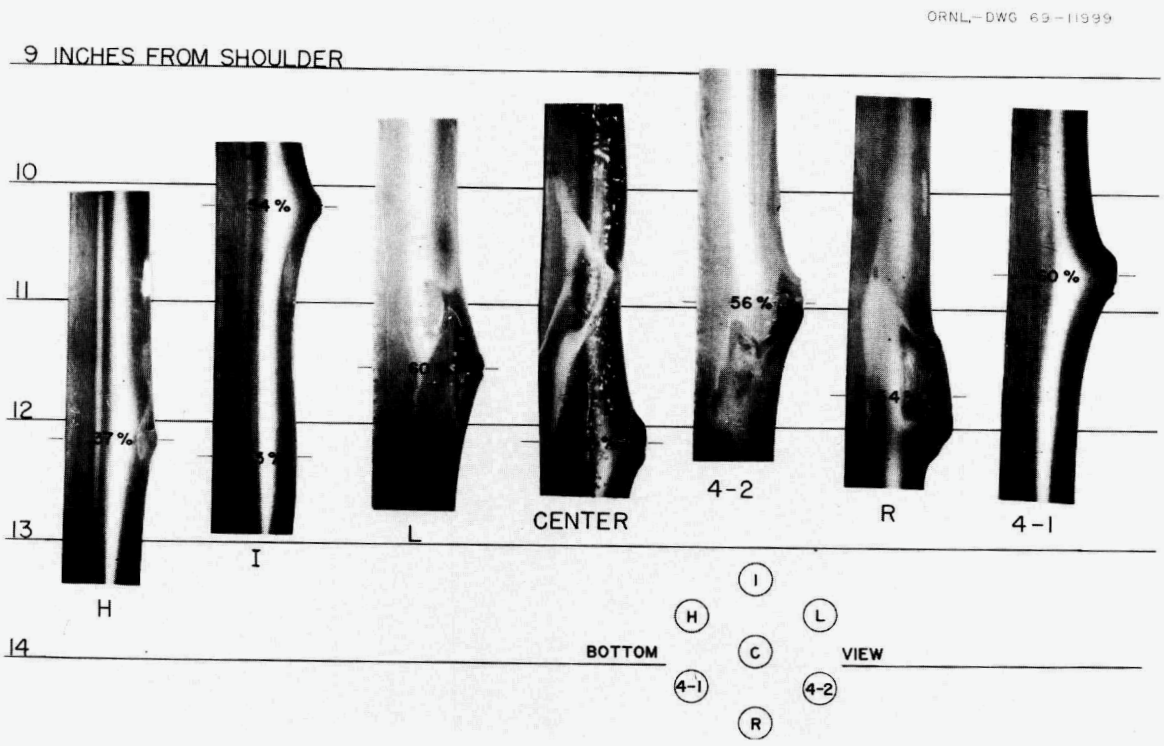

Fig. 4.18 Similar to Fig. 4.17, Except that the Views are in Elevation.

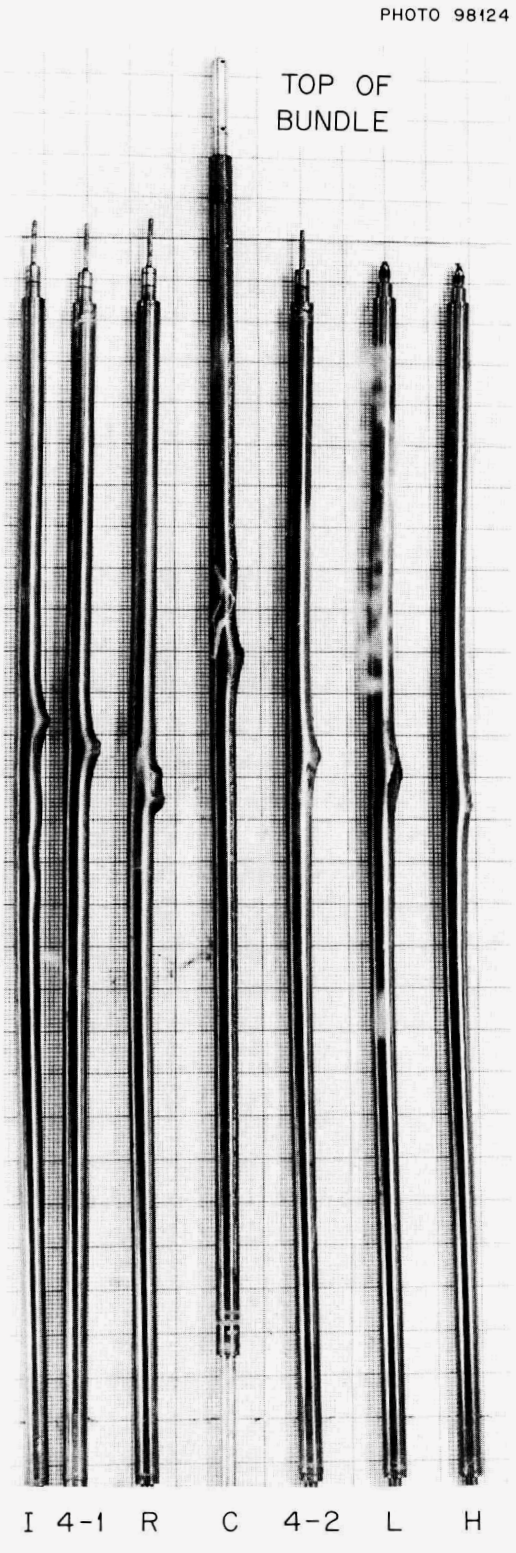

Fig. 4.19 Photograph of the Rods Taken Against the Large Sheet of Graph Paper to Show Maximum Bowing. The Rods are I, 4-1, R, Center, 4-2, L and H, from right to left.

rotated to allow further bowing to take place, or else bowed initially in a direction parallel to the circumference of the bundle. This is consistent with the remarks concerning rod rotation in the previous paragraph.

As was shown in the montages in Figs. 4.17 and 4.18, the amounts of swelling and the appearances of the rupture regions varied greatly among the seven rods. All of the rods were prepressurized with helium gas to simulate fission gas build-up. The pressures varied as follows: Rods 4-1, 4-2, R and the center rod had 215 psi initially; rod L had 207 psi; rod H had 133 psi and rod I had 115 psi. Pending metallographic evaluation it can be generally stated that the lower the initial pressure, the smaller the rupture size and the smaller the amount of swelling. It is impossible at this time to evaluate all the factors relating to the rupture characteristics of the rods.

4.5 Calculation of Flow Channel Obstruction from Rod Swelling

A somewhat pessimistic set of data has been obtained for rod swelling based on the assumptions illustrated in Fig. 4.20. The original rod was assumed to swell while maintaining a circular cross section and then to burst as shown in the figure. Measurements were made at 1/2 inch intervals (true scale) of the apparent diameters of the rods shown in plan and elevation in Figs. 4.17 and 4.18. The cross-sectional area increases were then calculated according to the equations in Fig. 4.20. The results are shown in Table 4.3 together with the estimated remaining flow area. Although the rods were tested in a triangular array in the TREAT capsule, the calculations for Table 4.3 are based on the square array that corresponds to present day light-water reactor practice. Such an array is shown in Fig. 4.21 together with the areas of interest to the calculations.

ORNL-DWG 69-11998

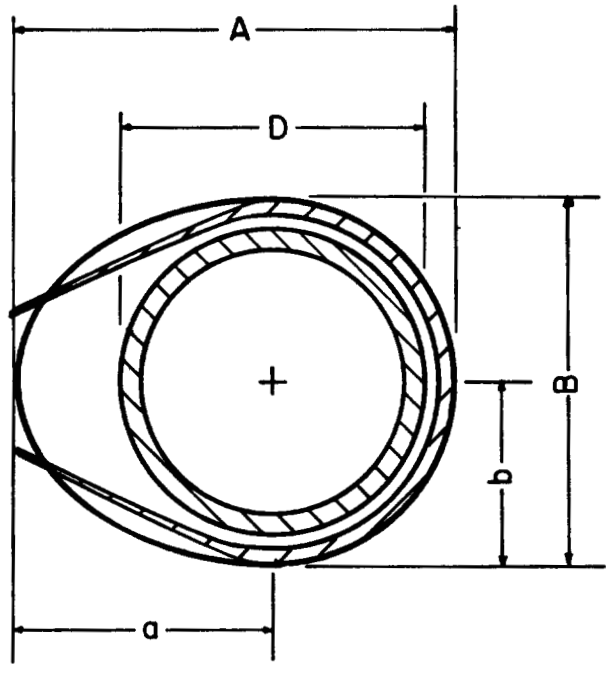

$$A_{Ellipse} = \Pi ab = \Pi(A - B/2)(B/2), \quad A_{Circle} = \Pi b^2 = \Pi(B/2)^2$$

$$A_{Egg} = \Pi/2 \left[(A - B/2)(B/2) + (B/2)^2 \right]$$

$$A_{Orig.\ circle} = \frac{\Pi D^2}{4}$$

$$\text{Area increase} = \frac{A_{Egg} - A_{Orig.}}{A_{Orig.}}, \ (\%)$$

Fig. 4.20. Diagram and Equations Illustrating the Assumptions Made in Calculating Cross-Sectional Area Increases for the Rods.

Table 4.3. Area Calculations for the TREAT Experiment

Distance from Upper Shoulder of Rod (in.)	Average Expanded Rod Area ($in.^2$)	Remaining Flow Area ($in.^2$)	Remaining Flow Area (% of Orig. Area)
10	1.460	0.719	60.5
10.5	1.562	0.617	51.9
11	1.640	0.539	45.4
11.5	1.676	0.503	42.3
12	1.681	0.498	41.9
12.5	1.497	0.682	57.4
13	1.360	0.819	68.9

The flow area remaining after expansion and bursting of the rods is plotted in Fig. 4.22 against the distance from the top shoulders of the rods. It is seen that, even with the pessimistic approach used in the calculations, the final flow area did not drop below 40% of the original area. Since, in the calculations, it was assumed that the areas within the flared lips of the ruptures were lost as flow areas and since such areas could probably still support some flow, it is probably safe to assume at least 50% of the original flow area remained.

4.6 Flux Profile Obtained From Gamma Scans of Outer Rods

A short section of the center fuel rod 15 in. below the shoulder was cut out for burnup analysis and metallographic examination. The remainder of the center rod and all six

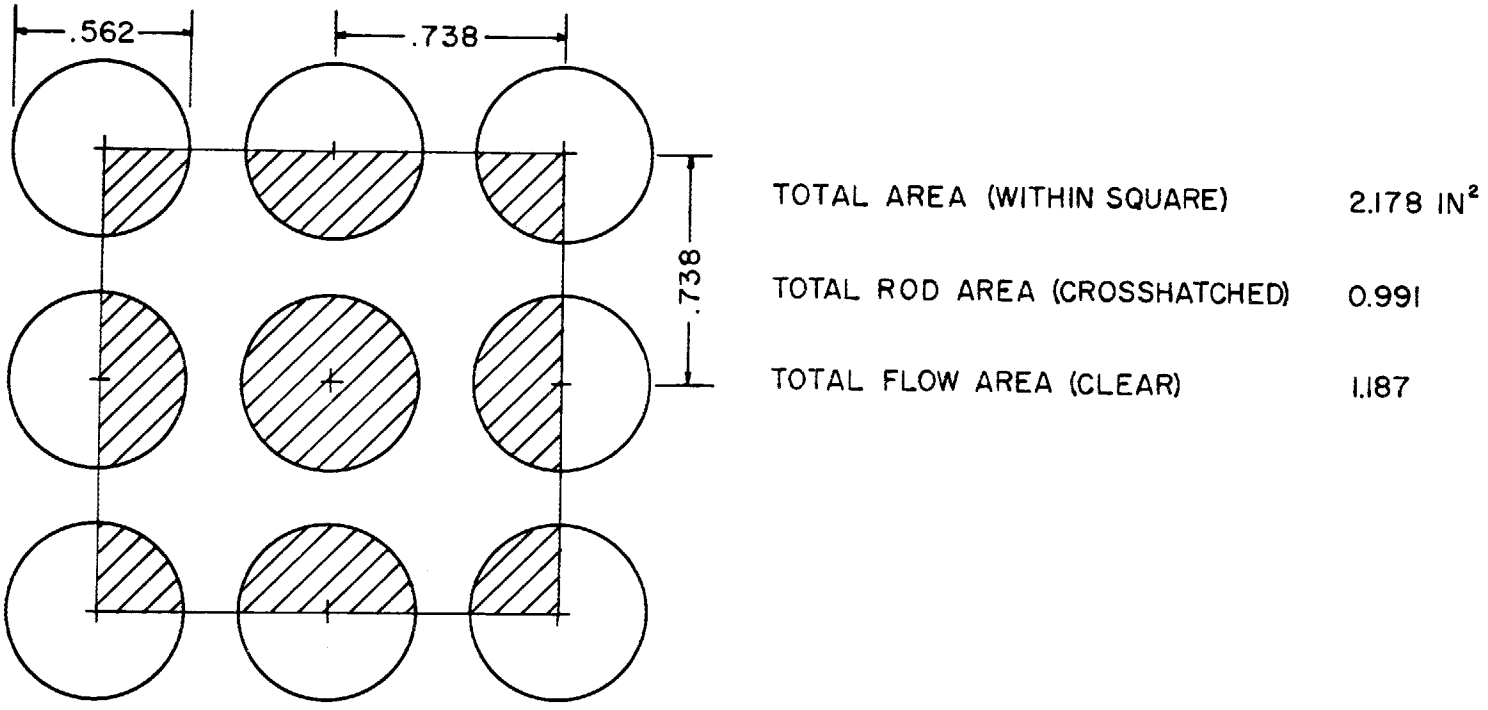

Fig. 4.21. Square Array Used in the Swelling Calculations.

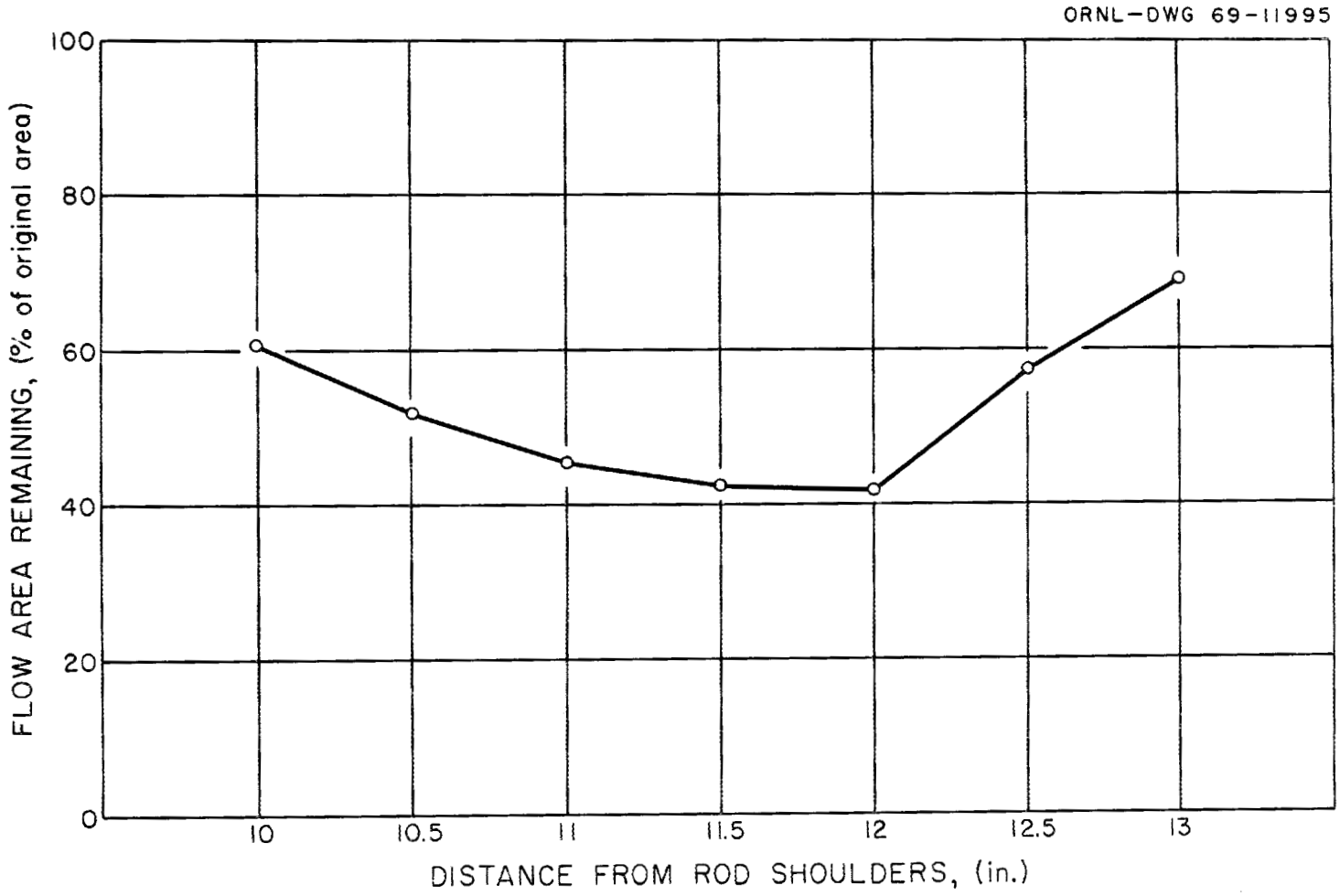

Fig. 4.22. Plot of Calculated Flow Area Remaining After the Rods had Ruptured Versus Distance From Upper Shoulders of the Rods.

outer rods were returned to ORNL where they will undergo further metallographic examination. The six outer rods were gamma scanned for flux profile and to look for fission products and fuel blown out from the center rod. Specific activity of the center rod fuel is about 10^4 higher than that of the outer rods. The greatest amount of "contamination" from the center rod was found on rod H in a zone from 12 to 8 inches below the top shoulder. Rod I had one-third as much contamination in a zone 12.5 to 9.5 in. below the top shoulder. Rod L had some contamination between 6.5 and 3.5 in. below the top shoulder.

The average flux profile found by the gamma scan is shown in Fig. 4.23 along with an unperturbed curve expected if a TREAT fuel element occupied the experiment location. Significant flux depression occurred in the lower half of the experiment from a heavy molybdenum liner placed there to hold and freeze melted Zircaloy cladding that might result from an accidental full-power TREAT transient. Now that precise reactivity data have been obtained, we can thin out and relocate the molybdenum liner to help flatten out the flux profile.

5.0 WORK IN PROGRESS

5.1 Further Analyses of FRF-1

Fission product analyses will continue including burnup of the center rod (from MTR irradiation) and outer rods (from TREAT). Fuel will be removed from the cladding permitting easy and accurate measurements of cladding characteristics in both the ruptured and unswollen regions. Calculations of heat loss from outer rods will be made.

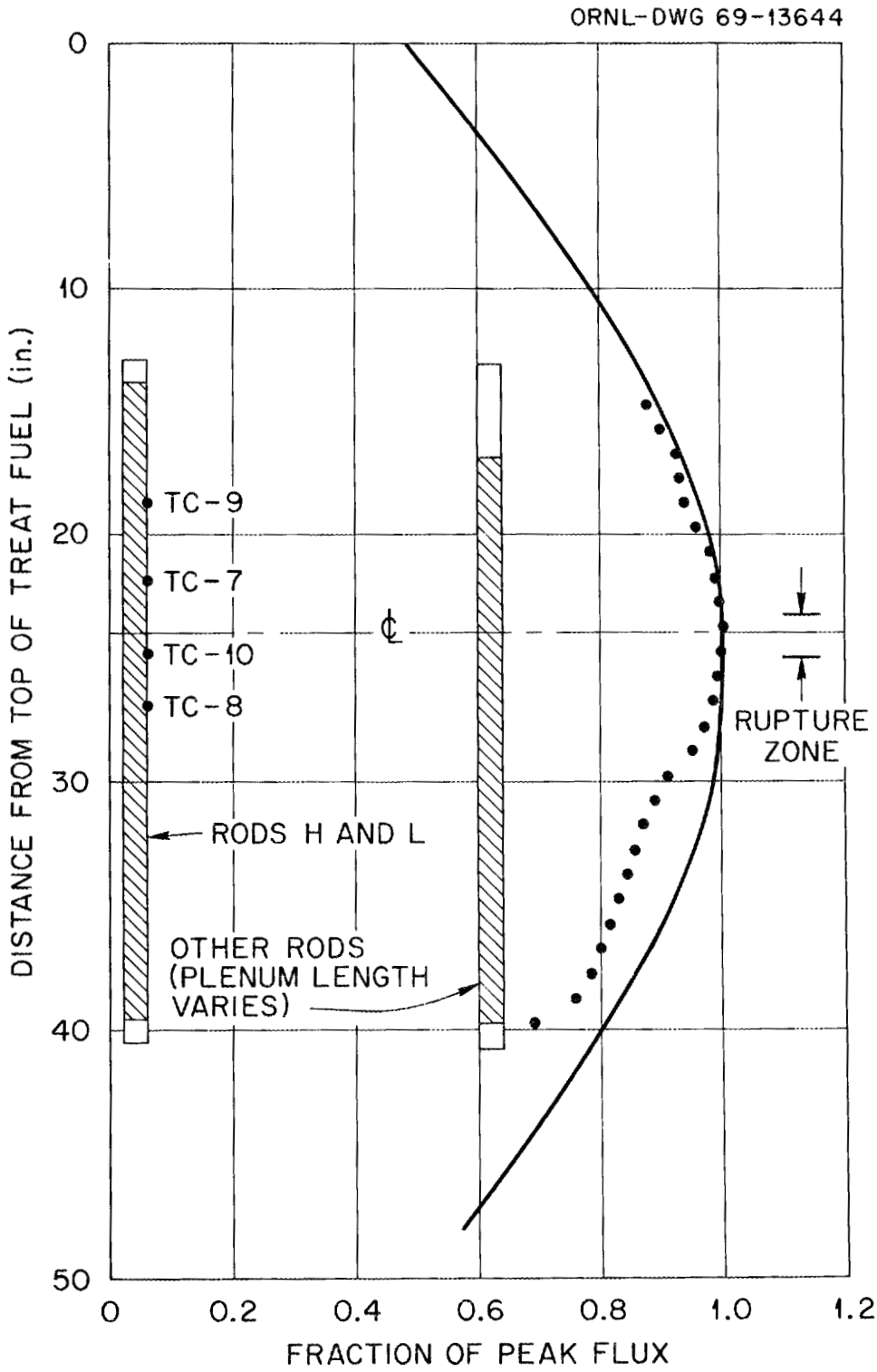

Fig. 4.23. Flux Profile and Thermocouple Location in Fuel Rod Failure Experiment FRF-1.

5.2 Plans for FRF-2

Experiment FRF-2 will use all Zircaloy-4 cladding on the 7-rod bundle. The center rod is now in the ETR for a planned 3000 Mwd/ton irradiation and is scheduled out Nov. 8. It was pressurized to 65 psia (25°C) with helium and we plan to use this same pressure in all outer rods. Twelve thermocouples will be placed on the rods to determine precise temperature differences. Two rods will be pressure-monitored, and the primary vessel pressure will also be recorded with fast-response equipment. A gold-plated heat-reflective sleeve will surround the rod bundle to test the effect of less heat loss from the outer rods. Only one filter pack will be used to allow space for raising the primary vessel 4 in. so that peak flux occurs lower on the rods away from the rod plenums. Two separate fission product collection units will be used as before downstream from the in-reactor equipment. The FRF-2 experiment is scheduled for January, 1970, and the same temperature rate of rise is planned. A new computer-controlled reactor control system is scheduled to be installed in TREAT by December, 1969, which will permit a higher maximum clad temperature for a longer time. The fuel rods will be pinned into place to prevent rotation during the test.

6.0 CONCLUSIONS AND RECOMMENDATIONS

The first TREAT fuel rod failure experiment, FRF-1, performed satisfactorily as designed. The experiment simulated the post-blowdown phase of a loss-of-coolant accident by using UO_2 pellets as the very realistic heat source in a 7-rod bundle. Fission products released from the center rod into the flowing steam atmosphere were collected and the samples are undergoing radiochemical analysis.

At this time only limited conclusions concerning the cladding behavior can be drawn from this experiment. More detailed evaluation must wait for metallographic examination of the rods.

In general, the rods appeared to behave in a ductile manner with considerable bulging taking place before rupture occurred. The rupture edges were thinned from the original wall thickness and, in the case of rod R, seem to be able to undergo bending without fracture. The fuel pellets, as seen through the ruptures, were unbroken except for the center rod. The ruptures were all toward the inside of the rod bundle indicating a higher cladding temperature away from the relatively cool Zircaloy sleeve that surrounded the bundle. It is probable that the cool sleeve reduced the amount of swelling of the rods and also acted as a restraint against bowing of the rods. The original clearance between the rods and the sleeve was approximately 1/16 inch and many of the rods bowed considerably more than this.

Preliminary calculations showed the coolant channel cross-sectional area to have been decreased a maximum of 58% by the swelling of the rods. If the rods had not been cooled by the sleeve it is probable that a larger amount of the channel would have been blocked. The rupture points of the rods made contact with adjacent tubes in most instances, but the tube surfaces did not appear to be in intimate contact over any appreciable distances. Again, it is possible that the sleeve acted as a restraint and that the rods separated when the bundle was withdrawn from the capsule.

Preliminary evaluation of the first test brings several considerations for changes to be made in future TREAT experiments:

1. More thermocouples are needed for a comprehensive evaluation of the temperature profiles in the bundle. Both axial and radial temperature gradients must be evaluated.

2. Heat losses from the outside rods to the surrounding sleeve should be curtailed either by a highly reflective sleeve or else by provisions for rapid heating of the sleeve to simulate surrounding fuel rods.

3. The surrounding sleeve should be enlarged to avoid interference with the rods.

4. Rotation of the rods should be prevented and positive axial positioning should be available.

5. The end restraints should be tailored to more closely approximate actual reactor conditions.

6. The cladding should be characterized with respect to wall thickness variations, texture and microstructural conditions.

7. Some means should be provided for maintaining the spatial relationships among the rods so that accurate post-test coolant channel measurements can be made.

REFERENCES

1. G. W. Parker and R. A. Lorenz, Rupture Tests of Irradiated Fuel Capsules, Nuclear Safety Program Annual Progress Report for Period Ending December 31, 1968, USAEC Report ORNL-4374, pp. 84-88, Oak Ridge National Laboratory.

2. G. W. Parker and M. F. Osborne, Out-of-Pile Experiments with Fuels Irradiated at High Heat Generation Rates, Nuclear Safety Program Annual Progress Report for Period Ending December 31, 1967, USAEC Report ORNL-4228, pp. 3-9, Oak Ridge National Laboratory.

3. T. C. Rowland, UO_2 Irradiation for ORNL Final Report, GEAP-5642, pp. 27-28, June 1968.

4. G. W. Parker, G. E. Creek, et al., Out-of-Pile Studies of Fission-Product Release From Overheated Reactor Fuels at ORNL, 1955-1965, USAEC Report ORNL-3981, pp. 75-83, July 1967, Oak Ridge National Laboratory.

ORNL-TM-2774

INTERNAL DISTRIBUTION

1-2. Central Research Library
3-4. ORNL – Y-12 Technical Library Doc. Ref. Sec.
5-14. Laboratory Records Dept.
15. Laboratory Records, RC
16. ORNL Patent Office
17. Nuclear Safety Information Center
18. R. E. Adams
19. G. M. Adamson, Jr.
20. S. E. Beall
21. G. E. Boyd
22. R. H. Bryan
23. W. B. Cottrell
24. C. M. Cox
25. G. E. Creek
26. J. E. Cunningham
27. F. L. Culler
28. R. J. Davis
29. W. K. Ergen
30. M. H. Fontana
31. S. H. Freid
32. J. H. Frye, Jr.
33. W. R. Grimes
34. W. O. Harms
35. M. R. Hill
36-40. D. O. Hobson
41. C. G. Lawson
42-44. R. A. Lorenz
45. H. G. MacPherson
46. C. J. McHargue
47. H. A. McLain
48. W. J. Martin
49. M. F. Osborne
50. G. W. Parker
51-55. P. L. Rittenhouse
56. D. A. Sundberg
57. R. D. Waddell, Jr.
58. G. M. Watson
59. J. R. Weir, Jr.

EXTERNAL DISTRIBUTION

60. H. W. Behrman, RDT, OSR, AEC, Oak Ridge National Laboratory
61-62. J. F. Boland, TREAT, Argonne National Laboratory, Idaho Falls, Idaho
63-67. G. O. Bright, WRSPO, Phillips Petroleum Company, Idaho Falls, Idaho
68. G. F. Brockett, Idaho Nuclear Corporation, Idaho Falls, Idaho
69. G. M. Brown, Southern Nuclear Engineering, Dunedin, Florida
70. S. H. Bush, ACRS, Pacific Northwest Laboratory, Richland, Washington
71-75. W. P. Chernock, Combustion Engineering, Windsor, Connecticut
76. R. J. Colmar, DRL, AEC, Washington
77. D. F. Cope, RDT, SSR, AEC, Oak Ridge National Laboratory
78. P. R. Davis, Phillips Petroleum Company Idaho Falls, Idaho

79. E. H. Davidson, Division of Reactor Development and Technology, AEC, Washington
80. Harold Etherington, ACRS, Jupiter, Florida
81. W. L. Faith, ACRS, San Marino, California
82. R. F. Fraley, ACRS, AEC, Washington
83. A. Giambusso, Division of Reactor Development and Technology, AEC, Washington
84. F. A. Gifford, Jr., ACRS, Atmospheric Turbulence and Diffusion Laboratory, Oak Ridge
85. J. E. Grund, Portland General Electric Company, Portland, Oregon
86-90. H. L. Hamester, Division of Reactor Development and Technology, AEC, Washington
91. S. H. Hanauer, ACRS, the University of Tennessee
92. J. M. Hendrie, ACRS, Brookhaven National Laboratory, Upton, N. Y.
93-95. Rudy Herzel, Idaho Nuclear Corp., Idaho Falls, Idaho
96-100. D. H. Imhoff, General Electric Company, San Jose, California
101. R. J. Impara, DRS, AEC, Washington
102. J. E. Irvin, Pacific Northwest Laboratory, Hanford, Washington
103. H. S. Isbin, ACRS, University of Minnesota, Minn.
104. R. O. Ivins, Argonne National Laboratory, Argonne, Illinois
105. E. E. Kintner, Division of Reactor Development and Technology, AEC, Washington
106. W. B. Klinger, Idaho Nuclear Corporation, Idaho Falls, Idaho
107. H. G. Mangelsdorf, ACRS, Short Hills, New Jersey
108. R. H. Meservey, Idaho Nuclear Corporation, Idaho Falls, Idaho
109-110. J. E. McEwen, DRS, AEC, Washington
111. H. O. Monson, ACRS, Argonne National Laboratory, Argonne, Illinois
112-113. D. L. Morrison, Battelle Memorial Institute, Columbus, Ohio
114. A. A. O'Kelly, ACRS, Littleton, Colorado
115. David Okrent, ACRS, Argonne National Laboratory, Argonne, Illinois
116. N. J. Palladino, ACRS, Pennsylvania State Univ., University Park, Pennsylvania
117. A. J. Pressesky, Division of Reactor Development and Technology, AEC, Washington
118-119. C. Robbins, Atomic Industrial Forum, Inc., New York, N. Y.
120. J.A.L. Robertson, Chalk River Nuclear Laboratories, AECL
121. J. B. Roll, Westinghouse Atomic Power Division, Pittsburgh, Pennsylvania
122. Morris Rosen, DRL, AEC, Washington
123-126. M. F. Sankovich, Babcock and Wilcox, Lynchburg, Va.

127. J. M. Simmons, Division of Reactor Development and Technology, AEC, Washington
128. E. E. Sinclair, Division of Reactor Development and Technology, AEC, Washington
129. W. R. Stratton, ACRS, Los Alamos Scientific Laboratory, Los Alamos, New Mexico
130. S. A. Szawlewicz, Division of Reactor Development and Technology, AEC, Washington
131. E. Veenard, Edison Electric Institute, New York, N. Y.
132. D. E. Williams, Idaho Nuclear Corporation, Idaho Falls, Idaho
133. L. J. Ybarronda, Idaho Nuclear Corporation, Idaho Falls, Idaho
134. C. W. Zabel, ACRS, University of Houston, Houston, Texas
135. J. O. Zain, Idaho Nuclear Corporation, Idaho Falls, Idaho
136. Manager, AEC Idaho Operations Office, Idaho Falls, Idaho
137. Laboratory and University Division, Oak Ridge Operations
138-152. Division of Technical Information Extension